

Astrophysical signals from the neighboring brane

Sergey G. Rubin^{a,b,1}

^c *National Research Nuclear University MEPhI (Moscow Engineering Physics Institute),
Kashirskoe shosse 31, Moscow 115409, Russia*

^d *N.I. Lobachevsky Institute of Mathematics and Mechanics, Kazan Federal University,
Kremlyovskaya ulitsa 18, Kazan 420008, Russia*

Abstract

In this paper, we consider the two-brane model and show that any field is settled on both neighboring branes, thus forming two independent effective fields with different masses. The hierarchy of the energy scales and the subsequent fine-tuning can be achieved for a brane populated by observers. The neighboring brane is thus populated by extremely massive fields. The electromagnetic field is uniformly distributed over the extra dimensions, preserving charge universality in 4D physics.

It is shown that the particles on different branes interact by exchanging photons and gravitons, which could explain the phenomena such as ultra-high-energy cosmic rays and dark matter. The latter consists of heavy electrons that are located on a brane free of the observers.

1 Introduction

The idea of multidimensional gravity is a vital tool for obtaining new theoretical results and explaining known phenomena ([1–4]). Over the course of several decades, numerous significant results have been achieved, and various concepts have been developed. The hierarchy problem is undoubtedly one of the most significant issues (see e.g. [5–7]). The problem of the small cosmological constant is discussed in a variety of papers, see e.g. [8; 9], while the concept of multidimensional inflation is discussed in detail in several sources, including [10–12]. These works assume the extra-dimensional metric is static and stabilization occurs on high-energy scales. The stabilization of extra space as a purely gravitational effect has also been studied in [13–15].

Analytical solutions allow for prompt study of the stability [16–18] of one-brane configurations in 5D space-time. The stabilization mechanism for the radion in two-brane models was proposed in [19]. The numerical stability of extra dimensions was discussed in our paper [20]. In our paper [21] we used an alternative method — transforming the initial equation into one resembling the Schrödinger equation.

For several decades, significant interest has been observed in theories concerning the localization of fields on a three-dimensional hypersurface, known as a brane, within a multidimensional spacetime. Akama was the first who introduced this concept [22]. The hypothesis of the thick brane was independently formulated by Rubakov and Shaposhnikov [23].

Thin branes, widely discussed in the literature, suffer from some intrinsic problems [24]. Therefore, despite hopeful results, they are gradually being replaced by branes with internal structure - thick branes [25–30]. The latter require special conditions to prove their existence and stability. This could be the choice of a special metric, including the warp factor [31] or a special form of the scalar field potential [29]. A purely geometrical approach based on $f(R)$ gravity in 5D is given in [32], where a considerable number of bibliographic references can be found.

In brane-world scenarios, the key issue is the localization of fields on branes and the recovery of effective 4D gravity. The localization of gauge and spinor fields on branes is a necessary element of any brane model and is a widely discussed topic in the literature. The solutions representing the tensor mode excitations in the presence of a brane are examined in [17; 33] with a focus on the stability problem.

The introduction of the warp factor in a D-dim metric [31] generalizes the analysis, especially in the fermion sector, as outlined in [34], which provides a detailed analysis of this subject in even-dimensional space-time. Fermions in other types of extra metrics are studied in [35; 36].

The two-brane ideology is often based on the well-known 5D Randall-Sundrum model (RS1), describing two 3D thin branes located at two fixed points of the orbifold. The model postulates a fixed distance between the branes, which is one of its disadvantages. A substantial amount of references can be found in [37–39]. The formation of multiple thick branes is considered in, e.g. [28; 40]. In this study, we base

¹e-mail: sergeirubin@list.ru

on the results of our paper [41] where a new class of branes was discussed. Our analysis there shows that one-brane metrics are exceptions rather than the norm, and we are particularly interested in the set of metrics that describe two-brane configurations. It is shown here that both branes are filled by the same sorts of fields because they have a common origin at the highest energies. In the course of energy reduction, a field is split into two effective fields with different masses depending on the branes properties. Particles located on different branes can interact by exchanging photons. This opens up the possibility of clarifying phenomena such as dark matter [42] and cosmic rays of the highest energies.

As was shown in [9], the Sandwich model of extra dimensions discussed here could serve as the basis for resolving the hierarchy problem, including the issue of the smallness of the cosmological constant.

The paper is structured as follows. In Section 2, we discuss the energy scales suitable for the formation of classical extra-dimensional metrics. Section 3 introduces the basis of the Sandwich model of extra dimensions. Section 4 discusses fermions, photons, and the Higgs field distribution over the extra dimensions. We show that the matter fields split between the two branes. Section 5 discusses observable signals from the inhabited brane. Finally, we offer a conclusion in Section 6. The Appendix contains the analysis in which cases the matter located on different branes can be described as independent fields.

2 Spreading of matter on branes in the course of their formation

The widely accepted inflationary paradigm implies that the formation of the physical laws takes place above the inflationary scale $H_I \sim 10^{14}\text{GeV}$. Therefore, actions describing fields dynamic, such as (13) appear at extremely high energies where the quantum fluctuations dominate. The Randall-Sundrum model with two branes (RS1 model) and its developments [43] use the second brane as the source of gravity. But there is an aspect which is usually omitted. Indeed, the static two-brane structure does not exist forever, but was formed at high energies. When the universe cools down, two processes occur simultaneously: the extra-dimensional metric describing the branes stabilizes and the fields are randomly settled on them. As a result, the matter fields must be present on all branes.

The two-brane structure is broken by external perturbations if the energy scale is higher than the inverse distance l between the two branes. So we can consider static metrics at the energies where the wavelengths of the 4D fluctuations are much larger than the extra-space size l_{extra} . The characteristic wavelengths at the de Sitter stage are of the order of the inverse Hubble parameter H^{-1} . Therefore, the estimation $H \equiv H_D \ll l_{extra}^{-1}$ provides us with the energy scales where the specific two-brane metric can be considered static.

The D-dim Planck mass m_D determines the highest possible energy scale. So the first limit is $l_{extra}^{-1} \ll m_D$. Another inequality can be found by using the inflationary concept. It was shown in [44] that a scale of compact extra dimensions cannot be larger than the inflationary scale, $l_{extra} \ll 1/H_I$, in order not to destroy the slow rolling during the inflation. Combining these inequalities, we get the interval for the extra-space scale variation

$$H_I \ll l_{extra}^{-1} \ll m_D$$

The whole picture looks as follows. The extra-dimensional metric is formed below the energy scale $m_D \sim 10^{18}\text{GeV}$, and is stabilized above the scale $H_I \sim 10^{14}\text{GeV}$. It remains static at lower energies. The initial fluctuations of the fields are responsible for the stochastic distribution of matter on both branes.

3 Two-brane metric. Sandwich model of extra dimensions

3.1 The model choice

The presence of at least two branes is necessary element of this study so that we will base on the model elaborated in [41]. In that study, we impose the extra-dimensional metric and show that a two-brane structure is formed under some assumptions which are not very restrictive. The metric is supposed in the form

$$ds^2 = e^{2\gamma(u)} [dt^2 - e^{2Ht}(dx^2 + dy^2 + dz^2)] - du^2 - r(u)^2 d\Omega_{n-1}^2, \quad (1)$$

where $d\Omega_{n-1}^2$ is the metric on a unit $n - 1$ -dimensional sphere. The radial extra coordinate $X^4 \equiv u$ and $X^\mu \equiv x^\mu$, $\mu = 0, 1, 2, 3$. The angular coordinate $X^5 = \theta$ varies in the finite region. Here we consider a 6D space so that $D = 4 + n$, $n = 2$ and the set of extra-dimensional coordinates is $y = \{X^4, X^5\} \equiv \{u, \theta\}$. We do not fix the limits of the radial coordinate u a priori. The Hubble parameter H is arbitrary.

Consider $f(R)$ gravity in a $D = 4 + n$ -dimensional manifold M_D :

$$S = \frac{m_D^{D-2}}{2} \int_{M_D} d^D X \sqrt{|g_D|} f(R), \quad f(R) = aR^2 + R + c, \quad (2)$$

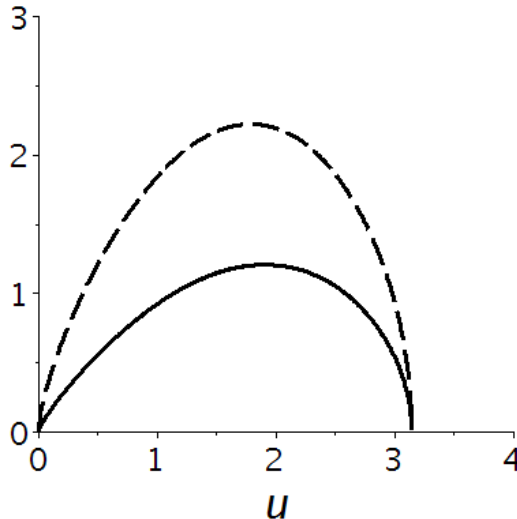


Figure 1: The typical metric functions, $\gamma(u)$ - solid line, $r(u)$ - dashed line. The interval is normalized so that the endpoints are $u_1 = 0$, $u_2 = \pi$ in the units $m_D = 1$. Their shapes depends on additional conditions and are characterized by zeros at the endpoints.

where $g_D \equiv \det g_{MN}$, $M, N = \overline{1, D}$, the $n - 1$ -dimensional manifold M_n is assumed to be closed, $f(R)$ is a function of the D -dimensional Ricci scalar R , and m_D is the D -dimensional Planck mass.

Remark that there are still no traces of branes, neither in the metric (1) nor in the gravity action (2). Nevertheless, branes are inevitably formed during the cooling of the universe. See [41]. The two-brane structure reveals as solutions of the classical equations

$$-\frac{1}{2}f(R)\delta_N^M + \left(R_N^M + \nabla^M \nabla_N - \delta_N^M \square_D\right)f_R = 0 \quad (3)$$

with $f_R = df(R)/dR$, $\square_D = \nabla^M \nabla_M$.

The static extra-dimensional metrics, being solutions of Eq.3, form an infinite set, as discussed in the papers [44–46]. It was shown there that their common form is characterized by two zeros of the metric functions $r(u_{1,2}), \gamma(u_{1,2})$, which is illustrated in Figs.1. The manifold is a compact n -dimensional space of a finite volume.

The classical equations are senseless at the distances m_D^{-1} where the quantum regime dominates. This statement holds for any classical system and is the reason why the space-time quantum foam exists at the Planck energy scale. In our case, this means that a brane width should be substantially larger than m_D^{-1} .

The thickness of the brane is related to the fields localization in its vicinity. As was shown in [9; 41], the classical field distributions along the extra coordinate u are characterized by two areas of localization. One can conclude that the model described above leads to the formation of the two-brane structure and we will refer to it as the Sandwich Model of Extra Dimensions (SMED).

3.2 The Planck mass

In this paper, we widely use the units $m_D = 1$ and it is instructive to restore its dimensionality at the final stage. The D -dimensional Planck mass m_D can be fixed by its connection to the known four-dimensional Planck mass m_4 . For this purpose, we make the necessary preparations here, starting with the representation of the Ricci scalar of 6D extra space in the form

$$R \equiv R_6 = e^{-2\gamma(u)}R_4(x) + R_2(u) + \mathcal{R}(u), \quad (4)$$

$$\mathcal{R} = -\frac{8}{r(u)}\gamma'(u)r'(u), \quad (5)$$

$$R_2(u) = -\frac{2r(u)''}{r(u)}, \quad (6)$$

where 2D extra metric presented in (1) has been taken into account. Here R_4 is the Ricci scalar of our 4D space and R_2 is the Ricci scalar of the extra space. We also assume that the distributions of matter

and metric functions over the extra dimensions depend only on the radial extra coordinate u . In this case, the action (2) takes the form

$$\begin{aligned}
S &= \frac{m_D^{D-2}}{2} \int_{M_D} d^D X \sqrt{|g_D|} f(e^{-2\gamma(u)} R_4(x) + R_2(u) + \mathcal{R}(u)) \simeq \\
&\frac{m_D^{D-2}}{2} \int_{M_D} d^4 x d^n y \sqrt{|g_D|} [f(R_2(u) + \mathcal{R}(u)) + e^{-2\gamma(u)} f_R(R_2(u) + \mathcal{R}(u)) R_4(x) + O(R_4^2)] \simeq \\
&\frac{m_4^2}{2} \int d^4 x \sqrt{|g_4|} [R_4(x) - 2\Lambda]
\end{aligned} \tag{7}$$

The 4D Planck mass m_4 is related to the D-dim Planck mass m_D as follows:

$$m_4^2 = m_D^{D-2} v_{n-1} \int du e^{2\gamma(u)} r(u) f_R(R_2 + \mathcal{R}), \tag{8}$$

where v_{n-1} is the volume of an $n - 1$ -dim sphere of unit radius

$$v_{n-1} = \frac{\pi^{\frac{n-1}{2}}}{\Gamma(\frac{n-1}{2} + 1)}. \tag{9}$$

The Planck mass m_4 is measured at the low energies, and we assume that the inequality $R_4 \ll R_2$ holds.

Let us estimate the value m_D . To this end, suppose that all dimensional values are of the order of m^D , so that

$$m_D \sim m_4 / \sqrt{v_{n-1}}. \tag{10}$$

The volume (9) has maximum $v_{n-1} \simeq 2500$ at $n \simeq 20$ which gives the estimation of the smallest value of $m_D \sim 0.02 m_4 \simeq 10^{17} \text{GeV}$. Here and below we suppose $m_D \sim 10^{17} \div 10^{18} \text{GeV}$ and the scale of the two-brane structure $l_{extra} \sim 10^{-14} \div 10^{-15} \text{GeV}^{-1}$ for the estimations. Other terms in (7) contribute to the vacuum energy density Λ , see discussion in [9], which is not used here. The knowledge of the metric functions $\gamma(u), r(u)$ as in Figure 1 permits to restore the 4D Planck mass m_D , see expression (10).

A non-trivial scenario arises if the number n of extra dimensions is large. In this case, the volume of extra dimensions (9) is a rapidly decreasing function of the number of extra dimensions. For example, $v_n \simeq 4 \cdot 10^{-15}$ at $n = 100$, so

$$m_D \sim 10^8 m_4 \sim 10^{27} \text{GeV}$$

The onset of the quantum regime occurs at a scale $1/m_D \sim 10^{-8}/m_4$, which is significantly smaller than the typically mentioned estimation $1/m_4$.

4 Fields splitting between two branes

Here we study the distributions of fields over the two branes and their features leading to observational consequences after the reduction to the 4D physics.

The space-time originated at the sub-Planckian energies, as is commonly assumed. This time period is characterized by strong fluctuations of the metric and the fields. The static extra-dimensional metrics, such as the two-brane structure, are formed at much lower energies and are accompanied by fields settling on the branes. As shown in the subsequent discussion, the physical parameters characterizing the behavior of a field are contingent upon the properties of the branes.

The reduction to 4 dimensions assumes integration over the extra coordinates. So we have to know the distributions of fields (scalars, fermions, vectors) within the extra dimensions. The suitable way of a field decomposition is as follows:

$$\Phi(x, y) = \Upsilon(x) Y_{cl}(y) + \sum_{k=0}^{\infty} \Upsilon_k(x) Y_k(y) \simeq \Upsilon(x) Y(y), \tag{11}$$

where $\{Y_k(y)\}$ is a set of orthonormalized functions. It is usually assumed that they satisfy the equation

$$\square_n Y_k(y) = \lambda_k Y_k(y), k = 0, 1, 2, \dots \tag{12}$$

The zero mode $Y_0(y) = 1$ satisfies this equation with $\lambda_0 = 0$. The function $Y_{cl}(y)$ is the classical solution to the field equation(s) provided that the derivatives in x coordinates of our space are neglected. This approximation holds if the wavelengths of the perturbations acting in our 3-dim space are much larger than a scale of the extra dimensions. It also means that the sum describing the field fluctuations along

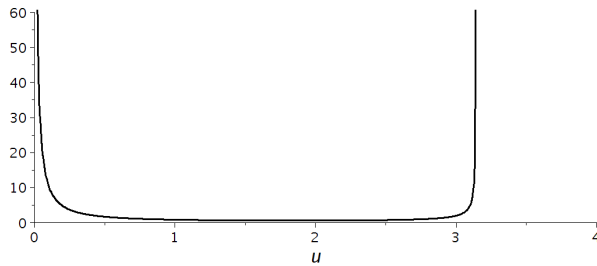


Figure 2: Fermion distribution over the extra dimensions. The metric functions are represented in Fig.1. The localizations near $u_1 = 0$ and $u_2 = \pi$ are evident.

the extra dimensions can be omitted. The function Υ is assumed to be endowed with group indices depending on the group representation of the field while the scalar function Y_{cl} is responsible for the distribution over the radial extra dimension. The fields are treated as trial functions in this research. This step does not involve any fine-tuning. The amplitude of the classical distributions, $Y_{cl}(u)$, is of the order of the D-dimensional Planck scale, m_D .

4.1 Fermions distribution over the extra dimensions

In this subsection we shortly remind the results of [41] concerning the distribution of fermions along the radial extra-dimensional coordinate u near the brane and in the bulk. General form of the free massless fermion action is

$$S_{fermion} = \int d^D z \sqrt{|g_D|} \bar{\Psi} i \Gamma^M D_M \Psi \quad (13)$$

The mass term is assumed to be generated by the interaction with the Higgs field. The particular form of the curved gamma matrices Γ^M and the covariant derivatives can be found in [31]. The useful discussion is also given in [47; 48]. The more thorough model in even dimensions is outlined in [34]. That paper studies conditions for decoupling the left and right chiralities of spinors. A useful discussion is also given in [47; 48]. A 6D spinor

$$\Psi = \begin{pmatrix} \xi_1 \\ \xi_2 \end{pmatrix} \quad (14)$$

acting in six dimensions is equivalent to a pair of 4-dimensional Dirac spinors ξ_1 and ξ_2 . As shown in [35], both 4D spinors, ξ_1 and ξ_2 , are equal in the s-wave approximation used in our approach. In this paper, we are interested in the spinor distribution over the extra dimensions. The spinor ψ is characterized by both spinor and group indices and functions within a six-dimensional framework. The field decomposition (11) in this case reads

$$\Psi(x, y) = \psi(x) Y_f(u). \quad (15)$$

Here $\psi(x)$ is endowed with spinor and group indices acting in 4-dimensional space.

This study focuses on the distribution of fields across the extra-dimensional coordinates rather than their reduction to four-dimensional physics. Consequently, our attention is directed towards the form of the function $Y_f(u)$. The particular distribution over the radial coordinate u is shown in Fig.2. The more detailed analysis is presented in [41]. The distribution has the sandwich-type structure with sharp peaks at the coordinates u_1 and u_2 and almost zero field value between them. The region proximate to the coordinate u_1 is designated brane-1, and the area near the coordinate u_2 is labeled brane-2.

4.2 Fields localization on branes

The existence of a region characterized by an extremely small amplitude of a field between the branes as in Fig.2, leads the bifurcation of the field into two effective fields with distinct parameters, which has profound implications.

The explanation on the "physical level" attracts the analogy with a scalar field behavior within the double-well asymmetric potential. When the energy of the system tends to zero, the field is concentrated near the potential minimums. In this case, the small-amplitude fluctuations around each of the minima are observed as free scalar particles with specific masses depending on the shapes of the minima.

The potential maximum between the two minima is responsible for the exponential attenuation of the field amplitude between the two minima. The overlapping integral of the fluctuations near distinct minima is small, so that these fluctuations do not interact with each other and can be considered as independent fields.

The same is true for fields concentrated near branes. The field near one brane does not "feel" the field located on the other brane due to the smallness of the overlapping integral. This is true for the zero mode. The KK mode excitations are forbidden if their typical wavelength $\sim 1/l_{extra}$, (l_{extra} is the distance between the branes) is much smaller than the electroweak scale.

This subject is also examined in detail in the Appendix. It is shown therein that a field situated on distinct branes can be treated as two independent fields, each with different parameters.

One can conclude that the field distributions near the two branes can be independently approximated by an appropriate sets of orthonormalized functions specific for each brane. These could be the sets built on the basis of harmonic oscillator, or the Coulomb set of wave functions for the hydrogen atom, for example. The general form of the wave function for the n-th energy level of a harmonic oscillator is as follows

$$\phi_n(u) = N_n H_n(\alpha u) e^{\alpha^2 u^2 / 2} \quad (16)$$

where N_n is the normalization factor, H_n is the Hermite polynomial of the n-th order, α is an arbitrary parameter. In the following, we will assume that all distributions are described by the set of functions $\phi_n(u - u_1)$ if they are located near brane-1, and functions $\phi_n(u_2 - u)$ if they are located near brane-2.

It is assumed that the observers are located at the brane-1. In this case, it is appropriate to choose the field distribution as a sum over the orthonormal basis (16)

$$Y_f^{(1)}(u) = \sum_n a_n \phi_n(u - u_1) \quad (17)$$

which reflects the fact of the field localization around $u = u_1$ (brane-1). A similar expression can be written for the fermion field located on brane-2 at $u = u_2$,

$$Y_f^{(2)}(u) = \sum_n b_n \phi_n(u_2 - u). \quad (18)$$

These functions quickly tend to zero if we limit ourselves by several terms in the sums. Thus, the distribution over the whole interval (u_1, u_2) can be approximated with good accuracy in the form

$$\Psi(x, u) = \Psi^{(1)}(x, u) + \Psi^{(2)}(x, u) = \psi_1(x) Y^{(1)}(u) + \psi_2(x) Y^{(2)}(u) \quad (19)$$

The first term has a sharp maximum at the brane-1, while the second term has a sharp maximum at the brane-2. This approximation is valid for all sorts of fields, provided they are localized on the different branes. Substitution (19) into the action (13) leads to the effective action for the two free fermions $\Psi^{(1,2)}$. The interference term $\Psi^{(1)} i D_A \Gamma^A \Psi^{(2)}$ is proportional to the overlapping integral

$$\int du \sqrt{g_n} Y_f^{(1)}(u) Y_f^{(2)}(u) \quad (20)$$

and hence is negligibly small. The main result of this section is the following: the fermions concentrated around different branes do not influence each other and can be considered as two different sorts of fermions.

4.3 Distribution of Higgs field across the extra dimensions

According to the Standard Model, the Higgs field is responsible for the fermion masses. In this subsection, we shortly remind of the Higgs field distribution along the extra dimensions referring the reader to the substantial discussion in [9]. As was shown there, the distribution of the Higgs field H_P over the extra coordinate u is governed by the scalar function $Y_H(u)$ which is the solution to the classical equation

$$- \left[\partial_u^2 + \left(4\gamma' + \frac{r'}{r} \right) \partial_u \right] Y_H(u) = \nu Y_H(u) - \lambda Y_H^3(u), \quad (21)$$

The initial conditions are specific to each causally disconnected 3D region below the horizon. Consequently, the field distributions are unique for each universe generated during the de Sitter stage. One of the solutions is depicted in Figure 3. As one can see, the Higgs field distribution is characterized by two peaks located on the branes and a nearly zero value in the region between them. In the Standard Model, the fermion masses are proportional to the Higgs vacuum average v_h . The latter is related to the Higgs mass m_h and self-coupling λ_h as

$$v_h = \frac{m_h}{\sqrt{2\lambda_h}}. \quad (22)$$

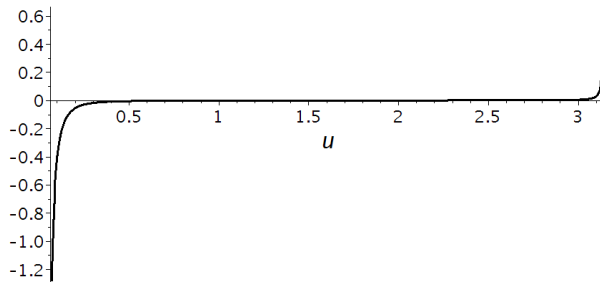


Figure 3: The Higgs field distribution over the extra dimensions. The metric functions are represented in Fig.1.

The expressions for the Higgs mass and the coupling constant as functionals of the function $Y_H(u)$ were obtained in [9].

$$m_h^2 = \mathcal{V}_{n-1} \int_{u_1}^{u_2} \left(-(\partial_u Y_H)^2 + \nu Y_H^2(u) \right) e^{4\gamma(u)} r^{n-1}(u) du, \quad (23)$$

$$\lambda_h = \mathcal{V}_{n-1} \int_{u_1}^{u_2} \lambda Y_H^4(u) e^{4\gamma(u)} r^{n-1}(u) du, \quad \mathcal{V}_{n-1} \equiv \int d^{n-1}y \sqrt{|g_{n-1}|} = \frac{2\pi^{\frac{n}{2}}}{\Gamma(\frac{n}{2})}. \quad (24)$$

It was declared from the beginning that the model is free from small values of the physical parameters. This means that the integrals as in (23) and (24) are of the order of unity if no special effort was made. The only fine-tuning is done here in the expression (23) to obtain the observable Higgs mass and its vacuum average, $v_h \sim 10^{-13} m_D$ (an estimation of $m_D \sim 10^{15}$ GeV is kept in mind). They have been made in the paper [9] by appropriate selection of the classical distributions $Y_H(u)$ over the extra dimensions.

In this paper, we take into account the brane structure of extra dimensions. It is assumed that the observers are settled on the brane-1. Hence, we have to choose the Higgs-1 field localized near $u = u_1$ (brane-1) and represent it as the sum over the orthonormal basis similar to the fermion approximation (15). This means that the integrand in expression (23) gives main contribution near the brane-1 where the function $\phi_n(u - u_1)$ has a sharp peak. The Higgs-2 field is located on brane-2 at $u = u_2$. It can be approximated as (18) which tends to zero near brane-1 and hence does not contribute to the observable parameter values.

The metric functions $\gamma(u), r(u)$ and the distribution $Y_H(u)$ are unique for each brane, so the parameters m_h, λ_h of the Higgs-1 and Higgs-2 fields are also different on branes 1 and 2. If we live on brane-1, these parameters must have observable values, see [49]. Hence, the values of the parameters m_h and v_h actual on the brane-1 need a strong fine-tuning, which was performed in [9]. In this research, we concentrate on the fields properties located on the brane-2 where the vacuum average $v_h^{(2)}$ of the Higgs-2 field remains uncertain varying in a wide range ($0 \div m_D \sim 10^{15}$ GeV) due to the absence of the fine-tuning.

4.4 Electromagnetic Field and Gravity between branes

In this subsection, we use the results obtained in [33; 41] to show that the electromagnetic field and the gravitational excitations are distributed uniformly between the branes.

We start with the action of the abelian gauge field and the standard form of its D-dimensional action, see e.g. [50]

$$S_{gauge} = -\frac{g_D}{4} \int d^D X \sqrt{|g_D|} g^{PM} g^{QN} F_{PQ} F_{MN},$$

$$F_{QN} = \partial_Q A_N - \partial_P A_Q. \quad (25)$$

Here g_D is the D-dimensional coupling constant. The classical equations

$$\partial_P (\sqrt{|g_D|} g^{PQ} g^{MN} F_{QN}) = 0 \quad (26)$$

are used to find the field distribution along the extra coordinate u . Keeping in mind expression (11) in the form

$$A^N(x, u) = a^N(x) Y_{em}(u) \quad (27)$$

equations (26) can be rewritten as follows ($n = 2$)

$$\begin{aligned} M = \mu : \quad & a^\mu \left[Y''_{em} + \left(2\gamma' + \frac{r'}{r} \right) Y'_{em} \right] = 0, \\ M = \theta : \quad & a^\theta \left[Y''_{em} + \left(4\gamma' - \frac{r'}{r} \right) Y'_{em} \right] = 0. \end{aligned} \quad (28)$$

Here, only nontrivial equations are written and condition $\partial_\mu \cdot = 0$ are used. The latter holds at the low energies where 4D wavelengths are much larger than the extra space scale. Evidently, $Y_{em}(u) = C_{em} = const$ is the unique solution to system (28) if $a^\mu, a^\theta \neq 0$ which means that the electromagnetic field is uniformly distributed between the branes. Charges located on one brane can emit the photons which are absorbed by charges on the other brane, see discussion in section 5.

Let us now discuss the gravitational perturbation over the extra coordinate u . The metric containing the tensor gravitational perturbations is of the form

$$ds^2 = e^{2\gamma(u)} (\eta_{\mu\nu} + h_{\mu\nu}) dx^\mu dx^\nu - du^2 - r(u)^2 d\phi^2 \quad (29)$$

$\eta_{\mu\nu} = diag(1, -1, -1, -1)$, $h_{\mu\nu} \ll \eta_{\mu\nu}$ where the perturbation $h_{\mu\nu}$ represents the tensor mode obeying the transverse-traceless gauge conditions

$$\eta_{\mu\nu} h^{\mu\nu} = 0, \quad \partial_\mu h^\mu_\nu = 0.$$

During this paper, we are interested in the main term of the decomposition (11) and represent the perturbations in the form

$$h_{\mu\nu}(x, u) = H_{\mu\nu}^{(0)}(x) Y_0(u) \quad (30)$$

Our aim is to find the distributions over the extra dimensions so that we put $H_{\mu\nu}^{(0)}(x) = const$ (it is assumed that the x -derivatives are small, or $\partial_\mu \cdot = 0$). After some algebra, see [33], equations for the linear tensor perturbations are reduced to a non-trivial equation

$$\left[\left(4\gamma' + \frac{r'}{r} \right) \partial_u + \partial_u^2 + \frac{\partial_u f_R}{f_R} \partial_u \right] Y_0(u) = 0. \quad (31)$$

for the tensor mode (30). One of the possible solutions of the equation (31) is $Y_0 = const$, as it should be for the zero mode. This means that the gravitational field is uniformly distributed between the two branes. Matter on one brane experiences the gravitational forces produced by matter on the other brane.

5 Manifestation of the second brane

In this section, we will briefly examine the possible observational implications of the hypothetical sandwich model of extra dimensions discussed in this paper. In the previous section, we have shown that

- Both branes are filled with similar types of fields.
- The particles on both branes can be exchanged by the photons and the gravitational waves.
- The hierarchy problem can only be solved on one brane. This means that complex structures like stars can only form on brane-1. Brane-2 is filled with a gas of heavy particles, in particular electrons.

The next subsection deals with the challenges of interpreting these particles as dark matter candidates. The most obvious property of dark matter is its extremely weak interaction with the electromagnetic field. So, we have to consider a D-dim extension of the SM action for the electron-photon interaction

$$S_{int} \equiv \alpha_D v_{n-1} \int \sqrt{|g_4|} d^4x \int_{u_1}^{u_2} du \sqrt{|g_n|} \bar{\Psi} \Gamma^N A_N \Psi. \quad (32)$$

Here α_D is a coupling constant in D dimensions and A_N is the gauge field. It is shown above that the gauge field is uniformly distributed over the extra dimensions, i.e. $A_N(x, y) = C_{em} a_N(x)$. Then action (32) can be reduced to the 4-dim action:

$$S_{int} \simeq \alpha_D v_{n-1} \int \sqrt{|g_4|} d^4x \int_{u_1}^{u_2} du \sqrt{|g_n|} (\bar{\Psi}_1 \Gamma^N A_N \Psi_1 + \bar{\Psi}_2 \Gamma^N A_N \Psi_2 + \bar{\Psi}_1 \Gamma^N A_N \Psi_2 + h.c.) \quad (33)$$

where $\Psi = \Psi_1 + \Psi_2$ and the functions Ψ_1, Ψ_2 are located on the brane-1 and brane-2 correspondingly, according to discussion in subsection 4.2. The next step is to substitute the decompositions $\Psi_{1,2} = \psi_{1,2}(x) \cdot Y_f^{(1,2)}(u)$ into action (33), to obtain

$$S_{int} = \int \sqrt{|g_4|} d^4x (\alpha \bar{\psi}_1 \gamma^\mu a_\mu \psi_1 + \alpha \bar{\psi}_2 \gamma^\mu a_\mu \psi_2 + \alpha_{12} \bar{\psi}_1 \gamma^\mu a_\mu \psi_2 + h.c.) \quad (34)$$

where expressions (15) and (19) have been kept in mind. We also used the fact that the extra space distribution of the fermions is included into the normalization of the wave functions $\psi_{1,2}$ and $\alpha = C_{em}^2 \alpha_D$. The observable coupling constant α is the same on both branes. The parameter α_{12} is proportional to the overlapping integral (20) and hence, is extremely small.

The first and the second terms in (34) contain the vertices describing the interaction of photons with "normal" electrons ψ_1 located at the brane-1 and "heavy" electrons ψ_2 on the brane-2. A photon emitted from the brane-1 can be absorbed by fermions located on brane-2, and vice versa. We will use this note below.

The third term represents the vertex containing both types of electrons in conjunction with the electromagnetic field. The transition of the heavy electron to another brane, accompanied by photon emission, is associated with this vertex.

5.1 Dark matter

One of the main goals of the cosmology is to understand the nature of the dark matter. Special efforts have been applied to explain the properties of this phenomenon and the origin of dark matter [51–58]. Many theoretical models as well as the observational evidences can be found in the reviews [59–61]. The idea of extra dimensions is also attracted in the framework of this discussion, [52; 62–64]. Some of them are treated the brane idea [65; 66] which is natural basis for production of small interacted particles. Our results reminds the concept of the mirror world [67; 68].

Let us return to the two-brane structure discussed above. We have shown that the observers could be on the brane-1, while the heavy electrons with the standard charge are on the brane-2. The question is, can these charged heavy electrons represent the dark matter? The main problem concerns their interaction with photons, which act equally on both branes [69]. So we have to estimate the Compton effect on brane-2, i.e. the photon scattering on the non-relativistic heavy electron. The cross section of the Compton effect depends on a particle mass m as

$$\sigma \sim \frac{1}{m^2} \sim 10^{-26} \text{cm}^2. \quad (35)$$

The second approximate equality is the known experimental result for the standard electron mass. The same cross section for the heavy electrons is smaller by the factor $(m_e/m_2)^2$ than the standard one. Here m_e and m_2 are the masses of the "normal" electron and the "heavy" electrons.

We can estimate the mass of the heavy electrons supposing that the cross section should be smaller than that for the Solar neutrino which is about 10^{-45}cm^2 ,

$$\sigma_2 \sim \frac{1}{m_2^2} \sim \frac{m_e^2}{m_2^2} \sigma_e \lesssim 10^{-45} \text{cm}^2. \quad (36)$$

It is easy to see that the heavy electron mass should be really large,

$$m_2 > 10^{10} m_e \sim 10^7 \text{GeV}, \quad (37)$$

where the value of σ_e is taken from (35). The mass estimate (37) for heavy electrons on brane-2 is derived from the assumption of the extremely weak interaction of charged heavy particles with photons. The mass is smaller than the maximum possible scale $\sim 10^{17} \text{GeV}$ where our study is carried out.

The next subsection discusses another way to estimate the heavy electron mass based on an observed phenomenon.

5.2 Ultra-high-energy cosmic rays

Ultra-high-energy cosmic rays (UHECR) of the energy 10^{11}GeV [70] are one of the most intriguing mysteries of modern astrophysics. So far, only several protons of such energy were definitely registered. Despite numerous attempts to explain this phenomenon, its origin remains largely unknown. The discussion on the origin of the high-energy photons of PeV energy can be found in [71].

The two-brane model discussed here provides us with a possible explanation of this phenomenon based on the heavy electron-positron annihilation into a pair of quarks. The part of action (34) contains three vertexes. The first term contains two fermion settled on brane-1 interacting with an electromagnetic field. The second one contains two fermions settled on the neighboring brane-2 coupled with the same electromagnetic field. So, the process describing the annihilation fermions on brane-2 into photon with the following creation of two other fermions on the brane-1 can be realized. The last term in (34) is proportional to the extremely small coupling constant α_{12} and is hardly significant. The energy ε of the emitted quarks on the brane-1 is of the order of the heavy electron mass m_2

$$\varepsilon \sim m_2 \quad (38)$$

provided that they are non-relativistic. This allows us to estimate the mass of the electrons settled on the brane-2 if we suppose that UHECR are the result of the heavy electron-positron annihilation,

$$m_2 \sim 10^{11} \text{ GeV}. \quad (39)$$

This value is consistent with the lower boundary limits (37). The small number of such events is due to the extremely small cross-section, as previously discussed.

A similar mechanism used to explain high-energy photons encounters difficulties. The highest observed photon energy is about 10^6 GeV, and the mass of a heavy electron must be of this order of the magnitude. However, this value is below the limit marked in (37), so some efforts should be applied to relate this effect to the dark matter.

6 Conclusion

Two-brane extra dimensions play an important role in theoretical research starting from the Randall-Sundrum model. In this research, we study the distribution of fields on the two-brane model which has been examined in [41]. This model has revealed its ability to explain the electroweak hierarchy problem, the restoration of the Starobinsky inflationary model [72], and the smallness of the cosmological constant [9].

Here we focus on the fields distribution on the branes. It is shown that any massive field, describing known particles, such as electrons, splits into two independent effective fields, localized on adjacent branes. This bifurcation process accompanies the evolution of the Universe from energy levels beyond the inflationary scale to the present-day energy state. The conditions under which the matter fields at neighboring branes are independent are discussed. At the same time, the gauge field is uniformly distributed in the extra dimensions, which preserves charge universality in 4D physics.

The hierarchy of the energy scales and the following fine-tuning are necessary phenomena for the formation of complex structures [73]. The selection of the physical parameters for the fine-tuning on a brane is a rather delicate process. It can be done only for one brane and it is reasonable to choose the brane-1 which is populated by observers. Brane-2 is then populated by all known sorts of particles with masses much heavier than those on brane-1. As the result, the matter on the brane-2 is incapable of containing complex structures like stars because of the lack of fine-tuning.

Some observational consequences are discussed. It is shown that matter particles disposed on the different branes can exchange via photons and gravitons. These effects could provide an explanation for the phenomena of dark matter and ultra-high-energy cosmic rays. Dark matter is located on a distinct brane than to the one on which the observers are situated. The extremely high mass of the heavy electrons on brane-2 is the key factor for the significant reduction of the Compton scattering cross section. This allows the heavy electrons to be considered as a component of dark matter and a source of ultra-high energy protons.

The Sandwich model of extra dimensions discussed here seems to be a promising framework that deserves further development. It could also serve as a basis for explaining phenomena such as the positron anomaly [74] and the smallness of the neutrino mass.

Acknowledgements

The author is grateful to K. Belotsky and R. Konoplich for fruitful discussions. The work was partly funded by the Ministry of Science and Higher Education of the Russian Federation, Project "New Phenomena in Particle Physics and the Early Universe" FSWU-2023-0073 The research presented in Sect.3,4 was also partially carried out in accordance with the Kazan Federal University Strategic Academic Leadership Program.

Appendix

A field disposed on two branes

Consider an action featuring the specific field $\zeta(x, y)$ along with its associated set of Lagrangian parameters $\{\lambda\}$, which include mass and coupling constants. At the highest energy levels, where $H \sim m_D$, this field is dispersed throughout the entire extra space. However, as the system's energy decreases to lower levels, the scenario changes. As shown in Fig.3, the field localizes near each brane. The function definition area is divided into three distinct regions. The first region, denoted as \mathcal{U}_1 , encompasses the extra-dimensional radial coordinate $u \in \mathcal{U}_1$ near brane-1, while another region includes the coordinate

$u \in \mathcal{U}_2$ near brane-2. The third region, denoted by \mathcal{U}_0 , acts as a separator between the two branes. Here, the field and its derivatives are negligible, and this part of action $S_0 \simeq 0$. The precise definition of the boundaries between the regions \mathcal{U}_1 , \mathcal{U}_0 , and \mathcal{U}_2 is not necessary.

Let us prove that this field is observed at low energy as two different fields characterized by different sets of parameters $\{\lambda\} \rightarrow \{\lambda_{1,2}\}$. The transition amplitude is calculated using the path-integral approach.

$$A = N \int D\zeta \exp(iS[\zeta]) \quad (40)$$

The action can be segmented into three components based on integration over the distinct regions \mathcal{U}_1 , \mathcal{U}_0 , and \mathcal{U}_2

$$S[\zeta] = \int d^4x d^n y \sqrt{|g|} L(\zeta(x, y)) = S_1 + S_0 + S_2 = \int_{u \in \mathcal{U}_1} d^4x d^n y \sqrt{|g_1|} L(\zeta_1) + \int_{u \in \mathcal{U}_0} d^4x d^n y \sqrt{|g_0|} L(\zeta_0) + \int_{u \in \mathcal{U}_2} d^4x d^n y \sqrt{|g_2|} L(\zeta_2) \quad (41)$$

The function ζ is denoted as ζ_1 in the region \mathcal{U}_1 and similarly for other regions. The second of the three integrals, S_0 , is essentially zero owing to the negligible field value and its derivatives between the branes (region \mathcal{U}_0).

Let us now break down the measure into three parts,

$$D\zeta = \prod_{x,y} d\zeta(x, y) = D\zeta_1 D\zeta_0 D\zeta_2 \quad (42)$$

$$D\zeta_k = \prod_{x,y,u \in \mathcal{U}_k} d\zeta_k(x, y); \quad k = 0, 1, 2. \quad (43)$$

We have introduced an extra index $k = 1, 2, 3$ to emphasize that there are three distinct sets of variables $\zeta(x, y)$ operating within the separate regions $\mathcal{U}_1, \mathcal{U}_0$, and \mathcal{U}_2 . Taking all this into consideration, the transition amplitude (40)

$$A = N \int D\zeta_1 D\zeta_0 D\zeta_2 \exp(iS_1[\zeta_1] + iS_0[\zeta_0] + iS_2[\zeta_2]) \\ = N' \int D\zeta_1 e^{iS_1[\zeta_1]} \int D\zeta_2 e^{iS_2[\zeta_2]} \quad (44)$$

is reduced to the amplitudes for the fields ζ_1, ζ_2 acting in the disconnected areas \mathcal{U}_1 and \mathcal{U}_2 . The normalization constant is changed as

$$N' = N \int D\zeta_0.$$

The integration here is performed over the spatial domain \mathcal{U}_0 , where $S_0 = 0$, with an appropriate level of precision.

Formally, transition amplitude (44) describes two independent fields ζ_1 and ζ_2 . The metric near the first brane does not coincide with the metric near the second brane. This is the reason for the different parameter values of the fields ζ_1, ζ_2 located near different branes.

The fields in the different branes do not feel each other. However, there are waves that can transfer energy between the branes. At the low energies, the wavelengths are much larger compared to the extra space scale and hence cannot be excited.

References

1. *Abbott R. B., Barr S. M., Ellis S. D.* Kaluza-Klein Cosmologies and Inflation // Phys. Rev. — 1984. — Vol. D30. — P. 720.
2. *Brown A. R., Dahlen A., Masoumi A.* Compactifying de Sitter space naturally selects a small cosmological constant // Phys. Rev. — 2014. — Vol. D90, no. 12. — P. 124048. — arXiv: [1311.2586 \[hep-th\]](#).
3. *Bronnikov K., Rubin S., Svadkovsky I.* High-order multidimensional gravity and inflation // Grav. & Cosm. — 2009. — Vol. 15. — P. 32–33.
4. *Chaichian M., Kobakhidze A. B.* Mass hierarchy and localization of gravity in extra time // Phys. Lett. — 2000. — Vol. B488. — P. 117–122. — arXiv: [hep-th/0003269 \[hep-th\]](#).

5. *Gogberashvili M.* Hierarchy problem in the shell universe model // Int. J. Mod. Phys. D. — 2002. — Vol. 11. — P. 1635–1638. — arXiv: [hep-ph/9812296](#).
6. *Randall L., Sundrum R.* Large Mass Hierarchy from a Small Extra Dimension // Phys. Rev. Lett. — 1999. — Vol. 83. — P. 3370–3373. — eprint: [arXiv:hep-ph/9905221](#).
7. *Arkani-Hamed N., Dimopoulos S., Dvali G. R.* The Hierarchy problem and new dimensions at a millimeter // Phys. Lett. — 1998. — Vol. B429. — P. 263–272. — arXiv: [hep-ph/9803315 \[hep-ph\]](#).
8. *Krause A.* A Small cosmological constant and back reaction of nonfinetuned parameters // J. High Energ. Phys. — 2003. — Vol. 09. — P. 016. — arXiv: [hep-th/0007233 \[hep-th\]](#).
9. *Bronnikov K. A., Popov A. A., Rubin S. G.* Multi-scale hierarchy from multidimensional gravity // Phys. Dark Univ. — 2023. — Vol. 42. — P. 101378. — arXiv: [2307.03005 \[gr-qc\]](#).
10. *Green A. M., Mazumdar A.* Dynamics of a large extra dimension inspired hybrid inflation model // Phys. Rev. D. — 2002. — Vol. 65, no. 10. — P. 105022. — eprint: [hep-ph/0201209](#).
11. *Bronnikov K., Rubin S., Svadkovsky I.* Multidimensional world, inflation and modern acceleration // Phys. Rev. D. — 2010. — Vol. 81. — P. 084010. — arXiv: [0912.4862 \[gr-qc\]](#).
12. *Fabris J. C., Popov A. A., Rubin S. G.* Multidimensional gravity with higher derivatives and inflation // Phys. Lett. B. — 2020. — Vol. 806. — P. 135458. — arXiv: [1911.03695 \[gr-qc\]](#).
13. *Günther U., Moniz P., Zhuk A.* Asymptotical AdS space from nonlinear gravitational models with stabilized extra dimensions // Phys. Rev. D. — 2002. — Vol. 66, no. 4. — P. 044014. — arXiv: [hep-th/0205148 \[hep-th\]](#).
14. *Günther U., Moniz P., Zhuk A.* Nonlinear multidimensional cosmological models with form fields: Stabilization of extra dimensions and the cosmological constant problem // prd. — 2003. — Vol. 68, no. 4. — P. 044010. — eprint: [hep-th/0303023](#).
15. *Arbuzov A., Latosh B., Nikitenko A.* Effective potential of scalar-tensor gravity with quartic self-interaction of scalar field // Class. Quant. Grav. — 2022. — Vol. 39, no. 5. — P. 055003. — arXiv: [2109.09797 \[gr-qc\]](#).
16. The structure of $f(R)$ -brane model / Z.-G. Xu [et al.] // Eur. Phys. J. C. — 2015. — Vol. 75, no. 8. — P. 368. — arXiv: [1405.6277 \[hep-th\]](#).
17. Multikink brane in Gauss-Bonnet gravity and its stability / N. Xu [et al.] // Phys. Rev. D. — 2023. — Vol. 107, no. 12. — P. 124011. — arXiv: [2201.10282 \[hep-th\]](#).
18. *Liu Y.-X., Yang K., Zhong Y.* de Sitter Thick Brane Solution in Weyl Geometry // JHEP. — 2010. — Vol. 10. — P. 069. — arXiv: [0911.0269 \[hep-th\]](#).
19. Cosmology of brane models with radion stabilization / C. Csaki [et al.] // Phys. Rev. D. — 2000. — Vol. 62. — P. 045015. — arXiv: [hep-ph/9911406](#).
20. *Nikulin V. V., Petriakova P. M., Rubin S. G.* Formation of Conserved Charge at the de Sitter Space // Particles. — 2020. — Vol. 3, no. 2. — P. 355–363. — arXiv: [2006.01329 \[gr-qc\]](#).
21. *Petriakova P., Popov A. A., Rubin S. G.* Flexible extra dimensions // Eur. Phys. J. C. — 2023. — Vol. 83, no. 5. — P. 371. — arXiv: [2303.04785 \[gr-qc\]](#).
22. *Akama K.* An Early Proposal of 'Brane World' // Lect. Notes Phys. / ed. by K. Kikkawa, N. Nakanishi, H. Nariai. — 1982. — Vol. 176. — P. 267–271. — arXiv: [hep-th/0001113](#).
23. *Rubakov V. A., Shaposhnikov M. E.* Do We live inside a domain wall? // Phys. Lett. — 1983. — Vol. 125B. — P. 136–138.
24. *Burgess C. P., Diener R., Williams M.* A problem with δ -functions: stress-energy constraints on bulk-brane matching (with comments on arXiv:1508.01124) // JHEP. — 2016. — Vol. 01. — P. 017. — arXiv: [1509.04201 \[hep-th\]](#).
25. *Bronnikov K., Meierovich B., Abdyrakhmanov S.* Global topological defects in extra dimensions and the brane world concept // Grav. Cosmol. — 2006. — Vol. 12. — P. 106–110.
26. *Chumbes A. E. R., Hoff da Silva J. M., Hott M. B.* A model to localize gauge and tensor fields on thick branes // Phys. Rev. D. — 2012. — Vol. 85. — P. 085003. — arXiv: [1108.3821 \[hep-th\]](#).
27. *Hashemi S. S., Riazi N.* Vacuum $f(R)$ thick brane solution with a modified Gaussian warp function // Annals of Physics. — 2018. — Vol. 399. — P. 137–148. — ISSN 0003-4916.
28. Thick branes in higher-dimensional $f(R)$ gravity / V. Dzhunushaliev [et al.] // Int. J. Geom. Meth. Mod. Phys. — 2020. — Vol. 17, no. 03. — P. 2050036. — arXiv: [1908.01312 \[gr-qc\]](#).

29. *Bazeia D., Lobão A. S.* Mechanism to control the internal structure of thick brane // Eur. Phys. J. C. — 2022. — Vol. 82, no. 7. — P. 579. — arXiv: [2206.10794 \[hep-th\]](#).
30. Smooth braneworld in 6-dimensional asymptotically AdS spacetime / J.-J. Wan [et al.] // JHEP. — 2021. — Vol. 05. — P. 017. — arXiv: [2010.05016 \[hep-th\]](#).
31. *Oda I.* Localization of matters on a string-like defect // Physics Letters B. — 2000. — Vol. 496, no. 1/2. — P. 113–121. — ISSN 0370-2693.
32. Localization of scalar field on the brane-world by coupling with gravity / H. Guo [et al.] // JHEP. — 2024. — Vol. 06. — P. 114. — arXiv: [2310.01451 \[hep-th\]](#).
33. Tensor Perturbations and Thick Branes in Higher-dimensional $f(R)$ Gravity / Z.-Q. Cui [et al.] // JHEP. — 2020. — Vol. 12. — P. 130. — arXiv: [2009.00512 \[hep-th\]](#).
34. *Wan J.-J., Liu Y.-X.* Localization of spinor fields in higher-dimensional braneworlds // JHEP. — 2023. — Vol. 12. — P. 033. — arXiv: [2303.06278 \[hep-th\]](#).
35. *Gogberashvili M., Midodashvili P., Singleton D.* Fermion generations from apple-shaped extra dimensions // Journal of High Energy Physics. — 2007. — Vol. 2007, no. 08. — ISSN 1029-8479.
36. Fermionic Kaluza-Klein modes in the string-cigar braneworld / D. M. Dantas [et al.] // Phys. Rev. D. — 2015. — Vol. 92, no. 10. — P. 104007. — arXiv: [1506.07228 \[hep-th\]](#).
37. *Olechowski M.* Stability of multibrane models. — 2024. — arXiv: [2408.15343 \[hep-th\]](#).
38. *Tanaka T., Montes X.* Gravity in the brane world for two-branes model with stabilized modulus // Nucl. Phys. B. — 2000. — Vol. 582. — P. 259–276. — arXiv: [hep-th/0001092](#).
39. *Feranie S., Arianto, Zen F. P.* Kaluza-Klein two-brane-worlds cosmology at low energy // Physical Review D. — 2010. — Vol. 81, no. 8. — ISSN 1550-2368.
40. *Bronnikov K. A., Meierovich B. E.* Global strings in extra dimensions: A Full map of solutions, matter trapping and the hierarchy problem // J. Exp. Theor. Phys. — 2008. — Vol. 106. — P. 247–264. — arXiv: [0708.3439 \[hep-th\]](#).
41. *Popov A. A., Rubin S. G.* Spontaneous branes formation. — 2024. — arXiv: [2408.14692 \[gr-qc\]](#).
42. *Song D., Murase K., Kheirandish A.* Constraining decaying very heavy dark matter from galaxy clusters with 14 year Fermi-LAT data // JCAP. — 2024. — Vol. 03. — P. 024. — arXiv: [2308.00589 \[astro-ph.HE\]](#).
43. *Randall L., Sundrum R.* An Alternative to compactification // Phys. Rev. Lett. — 1999. — Vol. 83. — P. 4690–4693. — arXiv: [hep-th/9906064 \[hep-th\]](#).
44. *Nikulin V., Rubin S. G.* Inflationary limits on the size of compact extra space // International Journal of Modern Physics D. — 2019. — Vol. 28. — P. 1941004. — arXiv: [1903.05725 \[gr-qc\]](#).
45. *Rubin S. G.* The role of initial conditions in the universe formation // Grav. & Cosm. — 2015. — Vol. 21. — P. 143–151. — arXiv: [1403.2062 \[gr-qc\]](#).
46. *Rubin S. G.* Scalar field localization on deformed extra space // Eur. Phys. J. — 2015. — Vol. C75, no. 7. — P. 333. — arXiv: [1503.05011 \[gr-qc\]](#).
47. *Appelquist T., Cheng H.-C., Dobrescu B. A.* Bounds on universal extra dimensions // Phys. Rev. D. — 2001. — Vol. 64. — P. 035002. — arXiv: [hep-ph/0012100](#).
48. *Randjbar-Daemi S., Shaposhnikov M. E.* Fermion zero modes on brane worlds // Phys. Lett. B. — 2000. — Vol. 492. — P. 361–364. — arXiv: [hep-th/0008079](#).
49. *Workman R. L.* [et al.]. Review of Particle Physics // PTEP. — 2022. — Vol. 2022. — P. 083C01.
50. *Dubovsky S. L., Rubakov V. A., Tinyakov P. G.* Is the electric charge conserved in brane world? // JHEP. — 2000. — Vol. 08. — P. 041. — arXiv: [hep-ph/0007179](#).
51. *Gani V. A., Dmitriev A. E., Rubin S. G.* Deformed compact extra space as dark matter candidate // Int. J. Mod. Phys. — 2015. — Vol. D24. — P. 1545001. — arXiv: [1411.4828 \[gr-qc\]](#).
52. *Burnell F., Kribs G. D.* The abundance of Kaluza-Klein dark matter with coannihilation // Phys. Rev. D. — 2006. — Vol. 73, no. 1. — P. 015001. — eprint: [arXiv:hep-ph/0509118](#).
53. *Hooper D., Profumo S.* Dark matter and collider phenomenology of universal extra dimensions // Phys. Rep. — 2007. — Vol. 453. — P. 29–115. — eprint: [arXiv:hep-ph/0701197](#).
54. *Khlopov M. Y.* Composite Dark Matter from 4-th Generation // Pis'ma Zh. Ehksp. Teor. Fiz. — 2006. — Vol. 83. — P. 3–6.
55. *Arbuzova E., Dolgov A., Singh R.* R^2 -Cosmology and New Windows for Superheavy Dark Matter // Symmetry. — 2021. — Vol. 13, no. 5. — P. 877.

56. *Belotsky K., Rubin S., Svadkovsky I.* Extended micro objects as dark matter particles // Mod. Phys. Lett. A. — 2017. — Vol. 32, no. 15. — P. 1740008.
57. Signatures of primordial black hole dark matter / K. M. Belotsky [et al.] // Mod. Phys. Lett. A. — 2014. — Vol. 29, no. 37. — P. 1440005. — arXiv: [1410.0203 \[astro-ph.CO\]](#).
58. *Berezinsky V., Dokuchaev V., Eroshenko Y.* Small-scale clumps in the galactic halo and dark matter annihilation // Phys. Rev. D. — 2003. — Vol. 68, no. 10. — P. 103003. — eprint: [arXiv:astro-ph/0301551](#).
59. Hadronic and Hadron-Like Physics of Dark Matter / V. Beylin [et al.] // Symmetry. — 2019. — Vol. 11, no. 4. — P. 587. — arXiv: [1904.12013 \[hep-ph\]](#).
60. *Arbey A., Mahmoudi F.* Dark matter and the early Universe: a review // Prog. Part. Nucl. Phys. — 2021. — Vol. 119. — P. 103865. — arXiv: [2104.11488 \[hep-ph\]](#).
61. *Misiaszek M., Rossi N.* Direct Detection of Dark Matter: A Critical Review // Symmetry. — 2024. — Vol. 16, no. 2. — P. 201. — arXiv: [2310.20472 \[hep-ph\]](#).
62. *Chu X., Hambye T., Tytgat M. H. G.* The Four Basic Ways of Creating Dark Matter Through a Portal // JCAP. — 2012. — Vol. 05. — P. 034. — arXiv: [1112.0493 \[hep-ph\]](#).
63. *Baltz E. A., Hooper D.* Kaluza Klein dark matter, electrons and gamma-ray telescopes // J. Cosmol. Astropart. Phys. — 2005. — Vol. 7. — P. 1. — eprint: [arXiv:hep-ph/0411053](#).
64. *Kahil M. E., Harko T.* Is Dark Matter AN Extra-Dimensional Effect? // Modern Physics Letters A. — 2009. — Vol. 24. — P. 667–682. — arXiv: [0809.1915 \[gr-qc\]](#).
65. *Boehmer C. G., Harko T.* Galactic dark matter as a bulk effect on the brane // Class. Quant. Grav. — 2007. — Vol. 24. — P. 3191–3210. — arXiv: [0705.2496 \[gr-qc\]](#).
66. *SHAHIDI S., SEPANGI H. R.* Braneworlds and dark matter // International Journal of Modern Physics D. — 2011. — Vol. 20, no. 01. — P. 77–91. — ISSN 1793-6594.
67. *Beradze R., Gogberashvili M., Sakharov A. S.* Binary Neutron Star Mergers with Missing Electromagnetic Counterparts as Manifestations of Mirror World // Phys. Lett. B. — 2020. — Vol. 804. — P. 135402. — arXiv: [1910.04567 \[astro-ph.HE\]](#).
68. *Dubrovich V. K., Eroshenko Y. N., Khlopov M. Y.* Production and evaporation of micro black holes as a link between mirror universes // Phys. Rev. D. — 2021. — Vol. 104, no. 2. — P. 023023. — arXiv: [2102.03028 \[astro-ph.CO\]](#).
69. Effects of electrically charged dark matter on cosmic microwave background anisotropies / A. Kamada [et al.] // Physical Review D. — 2016. — Vol. 95. — P. 023502.
70. Review of particle physics / S. Navas [et al.] // Phys. Rev. D. — 2024. — Vol. 110, no. 3. — P. 030001.
71. Clusters of black holes as point-like gamma-ray sources / K. M. Belotsky [et al.] // Astropart. Phys. — 2011. — Vol. 35. — P. 28–32.
72. *Starobinsky A. A.* A New Type of Isotropic Cosmological Models Without Singularity // Phys. Lett. — 1980. — Vol. B91. — P. 99–102.
73. *Donoghue J. F.* The fine-tuning problems of particle physics and anthropic mechanisms // Universe or Multiverse? / ed. by B. Carr. — Cambridge University Press, 2007. — P. 231.
74. *Belotsky K. M., Kirillov A. A., Solovyov M. L.* Development of dark disk model of positron anomaly origin // Int. J. Mod. Phys. D. — 2018. — Vol. 27, no. 06. — P. 1841010. — arXiv: [1802.04678 \[astro-ph.HE\]](#).